Excited and ionic states of formamide: an excited-state photoelectron spectroscopy and ab initio study.

ter Steege, D.H.A.; Lagrost, C.; Buma, W.J.; Leigh, D.A.; Zerbetto, F.

DOI
10.1063/1.1513456
Publication date
2002

Published in
Journal of Chemical Physics

Excited and ionic states of formamide: An excited-state photoelectron spectroscopy and *ab initio* study

D. H. A. ter Steege, C. Lagrost, and W. J. Buma[a)]
University of Amsterdam, Faculty of Science, Institute of Molecular Chemistry, Nieuwe Achtergracht 127-129, 1018 WS Amsterdam, The Netherlands

D. A. Leigh
Department of Chemistry, University of Edinburgh, The King's Buildings, West Mains Road, Edinburgh EH9 3JJ, United Kingdom

F. Zerbetto
Dipartimento di Chimica "G. Ciamician," Università degli Studi di Bologna, V. F. Selmi 2, 40126 Bologna, Italy

(Received 3 June 2002; accepted 20 August 2002)

High-resolution excited-state photoelectron spectroscopy has been applied to unravel the spectroscopic and dynamic properties of the excited states of formamide populated by two- and three-photon excitation. In combination with *ab initio* calculations, this approach has led to various reassignments of previously observed states, and to the observation of new states. One of the aspects that particularly emerges from the present study is the important role of vibronic coupling, which leads to states of heavily mixed character. Projection on the ionic manifold—as is done in our studies—is, however, able to determine the various contributions of the wave function. Our studies have enabled us as well to resolve an apparent disagreement concerning the values of the ionization energies of the ground and first excited state of the radical cation. We find here adiabatic values of 10.233 ± 0.008 and 10.725 ± 0.020 eV, respectively. A final issue our studies shed light on concerns the vibrational properties of the ground state of the radical cation. © *2002 American Institute of Physics.* [DOI: 10.1063/1.1513456]

I. INTRODUCTION

Because of the presence of the amide group in biologically important molecules and because it is the repeat unit in industrially important polymers, it is generally recognized that a full understanding of its electronic properties is important. Formamide is the simplest compound containing this chromophore and thus the most natural model to be studied. We have an additional interest in formamide and related molecules because of our involvement in an experimental research program that is directed toward the study of amide-based catenane and rotaxane systems. These are a class of highly versatile molecular systems that offer great promise for the design of materials with user-defined properties.[1–5] Formamide is the simplest chromophore present in their building blocks and the study of its electronic states is therefore a prerequisite for the gas-phase study of larger fragments present in these systems.

Formamide is a planar molecule of C_s symmetry. Its electronic ground-state configuration is given by $\ldots(7\sigma)^2(8\sigma)^2(9\sigma)^2(1\pi)^2(2\pi)^2(10\sigma)^2(3\pi^*)^0$, or in terms of molecular orbitals of C_s symmetry, by the $\ldots(7a')^2(8a')^2(9a')^2(1a'')^2(2a'')^2(10a')^2(3a'')^0$ configuration.[6] As far as the doubly occupied orbitals are concerned, the most relevant can be characterized as follows: the $1\pi\,(1a'')$ orbital is delocalized and totally bonding, the nonbonding $2\pi\,(2a'')$ orbital has an electron density on the oxygen and nitrogen atoms, and the nominally nonbonding $10\sigma\,(10a')$ orbital is mostly localized on the oxygen atom and therefore often designated as the n_O orbital. The $3\pi^*\,(3a'')$ orbital is antibonding and is of importance when low-lying electronically excited states are considered. The vibrational properties of the ground state have been investigated in the gas phase and in low-temperature noble-gas, nitrogen, and CO matrices with ir and Raman spectroscopy.[7–12] These properties and the structural properties of the molecule in its electronic ground state have also been the subject of several theoretical studies.[13–15] Although the bond lengths and bonding angles of the ground-state structure of formamide have been well characterized in various microwave,[16–19] gas-phase electron-diffraction,[20] and vibration–rotational studies,[21] the planarity of the molecule has for quite some time been the subject of debate,[12,22,23] in particular in relation to the possibility of a nonplanar peptide unit and in relation to the amide resonance model.

The two highest occupied molecular orbitals, n_O and 2π, have been reported to be very close in energy[6,24,25] with the general consensus nowadays that the n_O orbital is above the 2π orbital. The ionic ground state D_0 is consequently assumed to derive from the removal of an electron from this n_O orbital, leading to the $X\,^2A'$ ionic state, whereas removal of an electron from the 2π orbital leads to the $D_1(1\,^2A'')$ ionic state. It is remarkable that there does not seem to be a similar agreement on the ionization energies. The by now generally

a)Author to whom correspondence should be addressed. Email address: wybren@science.uva.nl

quoted values for the adiabatic value of D_0 are 10.13 eV (Ref. 26) and 10.15 eV (Ref. 27), while for D_1 values of $\leqslant$10.52 eV (Ref. 26) and 10.40 eV (Ref. 27) are taken. Strangely enough, however, there is in the literature also reported a valence-electron spectrum with a resolution that is superior to all other reported spectra. In that study it is concluded that the adiabatic binding energy of the $n_O(10a')$ orbital is 10.226 eV, and that of the $2\pi(2a'')$ orbital $\leqslant$10.699 eV.[28] Although theoretical calculations in general show support for the order mentioned above, the order still remains ambiguous as the calculating energies are so close, and moreover, rather sensitive to the level of the calculation and the molecular geometry. In the present study we will settle this issue by a combination of experimental methods such as threshold ionization, nonresonant two-photon ionization, and excited-state photoelectron spectroscopy on the one hand, and theoretical methods on the other hand.

The electronic absorption spectrum of formamide has been measured by several groups.[6,24,29,30] Five bands, historically labeled as *W*, R_1, V_1, R_2, and *Q*, have been identified in this spectrum. A weak n_O-$3\pi^*$ (*W* band) has been placed at 5.8 eV. A recent vacuum-ultraviolet (vuv) electron energy loss spectroscopic (EELS) study[6] places the 2π-$3\pi^*$ valence transition (V_1) at 7.36 eV. This study has identified two Rydberg states at 6.70 eV (R_1) and at 7.72 eV (R_2), and proposed a large number of assignments for other weak features in terms of Rydberg states converging primarily upon D_0, but in some cases also in terms of Rydberg states converging upon D_1. Originally the *Q* band at 9.2 eV was assigned as resulting from the 1π-$3\pi^*$ excitation, but it would now seem that it arises from the superposition of transitions to several Rydberg states.

Excited-state photoelectron spectroscopy has shown to be a powerful tool to characterize excited states.[31] The essence of the technique is that the electronic and vibrational wave functions of an excited state, populated in a one-photon or multiphoton excitation process, are projected onto the rovibronic manifold of the radical cation. In general, it is seen that this projection can be done well on the vibrational manifold of the ground state D_0 of the radical cation. *Ab initio* techniques, and in particular density funtional theory (DFT) methods, have by now become so advanced for the ground state of the radical cation that the identification of the final state of such a ionization process—as far as the ion is concerned—can be done quite reliably. This thus opens up the door to a detailed characterization of the state that was ionized in terms of ionic wave functions, and leads the way to its identification. In several studies we have by now shown the kind of detail that can be reached. For example, in similar studies on the excited-state manifold of acetone,[32] we demonstrated that considerable reassignments needed to be done of spectra that for a long time were considered as ''solved.'' One other aspect that emerged from that particular study was how well wave functions could be resolved in terms of vibronically interacting states using the technique of excited-state photoelectron spectroscopy. Not only small molecular systems are amenable to these kinds of analyses; for 1,1′-bicyclohexylidene, for example, these techniques allowed us to propose a solution to a long-standing problem concerning the apparent presence of two low-lying valence states while only one would *a priori* have been expected.[33]

In the present study we have investigated with these experimental techniques and with *ab initio* DFT calculations the spectroscopy and dynamics of excited states of formamide. These states were populated employing two- as well as three-photon excitation, which, to our knowledge, is the first time that these states have been investigated with multiphoton excitation. We will show that our approach enables us to assign unambiguously the resonant features in these spectra. As a consequence, we find that previously proposed assignments need to be revised, and can extend considerably our knowledge about the excited-state and ionic manifold of this molecule.

II. EXPERIMENTAL AND THEORETICAL DETAILS

The setup employed in the present experiments has been described in detail previously[34,35] and will therefore only be summarized here. Two- and three-photon excitation spectra as well as excited-state photoelectron spectra have been measured using a laser system consisting of a XeCl excimer laser (Lumonics HyperEx-460) producing 10-ns pulses with a maximum energy of 200 mJ per pulse and typically used at a repetition rate of 30 Hz, in combination with a pulsed dye laser (Lumonics Hyperdye-500) running on several laser dyes. For the three-photon excitation experiments this dye laser operated on the Coumarine dyes C540A, C500, C480, C460, and C440 as well as Exalite 428 and 416, whereas for the two-photon excitation experiments DCM, Rhodamine 610, and Rhodamine 590 were used. In the latter experiments the dye laser output was frequency doubled using an angle-tuned potassium dihydrogen phosphate (KDP) crystal. The resulting excitation light was focused by a 25-mm quartz lens into the ionization region of a so-called magnetic bottle spectrometer, which is a slightly modified version of the ''2π analyzer'' designed by Kruit and Read[36] that has been interfaced with a pulsed molecular beam. In the ionization region of this spectrometer, the trajectories of the electrons produced in a laser shot become parallel after being subject to a strongly diverging magnetic field. After detection by a pair of microchannel plates, the signal is stored in a 500-MHz digital oscilloscope (Tektronix TDS540), which is connected to a personal computer.

An excitation spectrum is constructed by monitoring the yield of all produced photoelectrons, or, alternatively, photoelectrons with selected kinetic energies, as a function of the laser wavelength. Photoelectron spectra are recorded by increasing in steps the retarding voltage on a grid surrounding the flight tube, and transforming each time only the high-resolution part of the time-of-flight spectrum. In this way, an optimum energy resolution of about 6–8 meV can be obtained for all kinetic energies, although in the present experiments typical resolutions of 10–15 meV were obtained. In Sec. III B experiments will be described in which photoelectrons were created with a very low kinetic energy. Under our standard experimental conditions, these photoelectrons

would not be detectable, and we therefore applied in those cases a small electric field on the ionization region by means of two grids mounted on the pole faces of the magnet in order to ''push'' these electrons into the flight tube. The energy scale of the photoelectrons (with and without extra electric field) and the laser wavelength were calibrated using multiphoton resonances of krypton or xenon.[37] Commercially available formamide (Aldrich, 99+% spectrophotometric grade) was used as supplied.

In the first instance, we tried to perform experiments employing the pulsed molecular beam. For such experiments it turned out necessary to heat the sample to obtain enough vapor pressure. As was also noticed before,[6] heating leads, however, to decomposition with ammonia (NH_3) as one of its products. Since under these conditions the multiphoton resonances from ammonia overwhelmingly dominated excitation and photoelectron spectra, the experiments were in the end carried out on formamide introduced into the spectrometer via an effusive beam.

The analysis of our excited-state photoelectron spectra required accurate knowledge of the harmonic force fields of the neutral molecule and of its radical cation in their electronic ground states S_0 and D_0, respectively. To this purpose, *ab initio* calculations of the equilibrium geometries and harmonic force fields have been performed at various levels. In particular, we have investigated if the form of the employed density functional[38–41] (B3LYP versus BLYP) and the inclusion of higher-angular-momentum basis functions—since these functions have been reported to be necessary for an accurate description of bending vibrations[42]—were of major influence. It was found that the (U)B3LYP/6-311+G* (Refs. 43, 44) level was appropriate for the information we wanted to recover, and the results of these calculations, which have been performed employing the Gaussian suite of programs,[45] will be reported here.

III. RESULTS AND DISCUSSION

A. Calculations

In excited-state photoelectron spectroscopy the vibronic wave function of an intermediate vibronically excited state is projected onto the vibrational manifold of one of the electronic states of the ion, in general the ground state D_0. When the excited state is a Rydberg state, one generally observes that this ionization process takes place with a predominant $\Delta v = v^+ - v' = 0$ propensity, i.e., the vibrational quantum numbers remain unchanged upon ionization. Knowledge of the state in which the ion is created thus immediately enables one to specify the vibrational content in the intermediate state. Since, as yet, there is virtually nothing known about the vibrational frequencies in the ground state of the radical cation of formamide, calculations have been performed to determine these frequencies.

Optimization of the molecular geometry in S_0 and D_0 under the condition of C_s symmetry leads to the geometrical parameters given in Table I. In a previous study, the ground state of the neutral molecule was studied employing the larger 6-311++G(2*d*,2*p*) basis set.[12] The results obtained in the present calculations nearly duplicate those results, and are in good agreement with the parameters as determined in experimental studies. The ground state of the radical cation derives in our calculations from the removal of an electron from the $10a'$ orbital, which is generally described as nonbonding and localized on the oxygen atom. The optimized geometry of the D_0 state indicates that the nonbonding character of the n_O orbital is only approximate: in particular the C═O and C—N bond lengths, as well as the hybridization of the carbon atom, are effected by the removal of an electron from this orbital.

TABLE I. Geometrical parameters (Å and degrees) of formamide in its neutral ground state S_0 and in the ground state D_0 of the radical cation.

	S_0 Experimental[a]	S_0 B3LYP/6-311+G*	D_0 UB3LYP/6-311+G*
C–O	1.219	1.212	1.263
N–C	1.352	1.360	1.298
H_1[b]–N	1.002	1.009	1.017
H_2[b]–C	1.098	1.106	1.104
H_3[b]–N	1.002	1.004	1.015
O–O–N	124.7	125.1	126.6
H_1–N–C	118.5	119.6	122.2
H_2–C–N	112.7	112.5	121.0
H_3–N–C	120.0	121.7	120.2
O–C–N–H_1	0.0	0.0	0.0
H_2–C–N–H_1	0.0	0.0	0.0

[a]Values taken from Ref. 19.
[b]H_1 and H_3 are *cis* and *trans*, respectively, to the formyl hydrogen atom H_2.

Table II reports the vibrational frequencies that are obtained from the calculation of the harmonic force field for both states. Previously, the planarity of formamide in S_0—and associated with this, the validity of the amide resonance model—has been subject of quite some debate that culminated in the theoretical study of Foragasi and Szalay.[23] In this study it was shown that the planarity of the molecule also comes out at a theoretical level, but that one needs to be cautious to employ an appropriate combination of electron correlation methods and basis set. From Table II it can be concluded that the present methodology is indeed suitable

TABLE II. Experimental and *ab initio* vibrational frequencies (cm^{-1}) of ground and ionic states of formamide.

Frequency		$X\,^1A'$[a] B3LYP	$X\,^1A'$[b] Expt.	$X\,^2A'$[a] B3LYP	$X\,^2A'$[c] Expt.
a'	ν_1	3596	3545	3509	
	ν_2	3466	3451	3400	3363
	ν_3	2856	2852	2904	
	ν_4	1738	1734	1648	
	ν_5	1596	1572	1572	1627
	ν_6	1379	1378	1304	
	ν_7	1230	1255	1155	1210
	ν_8	1028	1030	1061	1073
	ν_9	552	565	479	481
a''	ν_{10}	999	1059	937	
	ν_{11}	624	602	702	
	ν_{12}	237	289	624	595

[a]Present calculations; frequencies scaled by 0.9676 (Ref. 53).
[b]Frequencies taken from Ref. 8.
[c]Present work; reported frequencies are averages over measured values in various photoelectron spectra.

TABLE III. Duschinsky matrix for the totally symmetric modes in the S_0 (rows, labeled by frequency in cm^{-1} and normal-mode numbering) and D_0 (columns, labeled by frequency in cm^{-1} and normal-mode numbering) states of formamide excluding CH and NH stretch vibrations. The last row gives the calculated intensities for ionization of the vibrationless level of S_0 to fundamental levels of totally symmetric modes in D_0 with $I[0_0^0]$ taken as 100.0.

	1648 (ν_4^+)	1572 (ν_5^+)	1304 (ν_6^+)	1155 (ν_7^+)	1061 (ν_8^+)	479 (ν_9^+)
1738 (ν_4)	**−0.52**	**0.64**	−0.37	0.39	0.14	0.06
1596 (ν_5)	**0.82**	**0.55**	−0.06	0.13	0.00	0.02
1379 (ν_6)	0.05	−0.24	0.39	**0.87**	−0.09	0.10
1230 (ν_7)	−0.19	0.42	**0.82**	−0.20	0.23	−0.14
1028 (ν_8)	0.12	−0.22	−0.12	0.00	**0.95**	−0.10
552 (ν_9)	0.00	0.01	0.09	−0.13	0.13	**0.98**
$I[(\nu_i)_0^1]/I[0_0^0]$	33.9	67.5	6.3	2.9	2.0	2.9

since no imaginary frequencies are found. As yet, we have tacitly assumed that the description of the normal modes remains the same upon ionization. The Duschinsky matrix for totally symmetric modes in S_0 and D_0 reported in Table III shows that in fact the opposite is true: a significant mode scrambling is observed, in particular for the ν_4 and ν_5 modes.

Apart from a comparison with experimental frequencies from our excited-state photoelectron spectra (*vide infra*), the validity of the present theoretical results can also be tested by comparison of the predicted photoelectron spectrum for ionization of S_0 to D_0 with experimental He(I) photoelectron spectra.[26–28] Within the Condon approximation and assuming that the electronic transition moment for the ionization process is independent of the photoelectron kinetic energy, the intensities in the photoelectron spectrum can be approximated by the Franck–Condon factors associated with ionization of the vibrationless level in the ground state S_0 to vibrational levels in D_0. The calculated intensities[46] for transitions to the six lower totally symmetric fundamental vibrational levels are given in Table III, from which it is concluded that significant activity of the 1572-cm^{-1} mode is expected in the photoelectron spectrum. This is indeed what is observed in the experimental spectrum that is dominated by a 197-meV (1590-cm^{-1}) progression. Previously this vibration was associated with ν_4^+, but the present calculations demonstrate that such a description is not correct. Activity is also predicted to occur in the ionic 1648-cm^{-1} mode, but in the reported spectra this activity overlaps with that of the 1572-cm^{-1} mode.

Since the equilibrium geometry and force field of Rydberg states converging upon D_0 generally closely resemble those of D_0, the Franck–Condon calculations also give a strong indication of the vibrational activity we may expect to see in their excitation spectra, as has been amply demonstrated in recent studies on nitrogen-containing cage compounds.[47–50] The present calculations thus tell us to anticipate dominant activity of the ν_5 and ν_4 modes. The calculated Duschinsky matrix shows at the same time that the distribution of activity over these two modes is rather susceptible to the precise magnitude of the normal-mode rotations. In this respect it is worth mentioning that even small differences in electronic structure—as occurring, for example, by the nominally nonbonding Rydberg electron—might lead to a different distribution of vibrational activity over the ν_4 and ν_5 modes in the excitation spectrum of a Rydberg state and the He(I) photoelectron spectrum of the ground state. Concurrently, this conclusion implies that photoelectron spectroscopy of excited Rydberg states may show nondiagonal ionization. Since the frequency difference between the ν_4^+ and ν_5^+ modes is of the order of our experimental resolution, this nondiagonal ionization will not be directly visible in the form of two separate peaks, but rather as a shift of a photoelectron peak to apparently lower or higher frequency in comparison to its position in other photoelectron spectra.

B. Ionization energies

As explained in the Introduction, the assignment and values of the first and second ionization potential have been the subject of discussion for quite some time. A major disturbing observation in this respect is that it is far from clear where the difference between the adiabatic values for D_0 of 10.13 eV (Ref. 26) and 10.15 eV (Ref. 27) on the one hand and 10.226 eV (Ref. 28) on the other hand comes from. In the present work, we have determined the adiabatic value of the lowest ionization potential in a number of ways. Our first results were obtained by applying direct two-photon ionization and observing the onset of ionization. To this purpose, an excitation spectrum was made of the two-photon energy region of 81 400–84 700 cm^{-1} (10.092–10.502 eV) employing electron detection. In this energy range the time-of-flight spectrum shows two electron peaks of which the kinetic energy changes proportional to the two-photon energy. By setting gates in the time-of-flight spectrum on these two photoelectron peaks, and compensating for changes in their kinetic energy upon scanning the excitation wavelength by adjusting the electric field in the flight tube—thus realizing that these photoelectrons always arrive at the same time at the detector—we were able to separate the excitation spectrum into contributions of ionization to the two ionization limits and determine these energies accurately. The resulting spectra are shown in Fig. 1. From the lower spectrum the adiabatic value of the lowest ionization energy is determined as 10.228 ± 0.015 eV, while for the second threshold a value of 10.419 ± 0.015 eV is found. The difference between the two values, 0.191 eV (1541 cm^{-1}), matches perfectly the vibra-

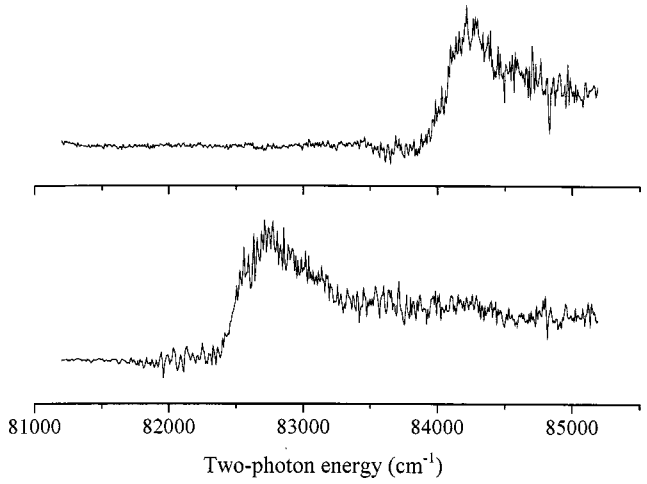

FIG. 1. Threshold two-photon ionization spectra of formamide. The lower spectrum displays the ionization channel associated in the present study with ionization to the vibrationless level of D_0, the upper spectrum with ionization to the $\nu_5^+=1$ level of D_0.

tional frequency of ν_5^+ and agrees well with the frequency of the vibrational progression observed previously in all He(I) photoelectron spectra.[26–28]

In a second experiment, direct two-photon ionization was performed at a one-photon energy of 43 500 cm^{-1} ($2h\nu=10.787$ eV). Kinetic-energy-resolved electron detection led in that case to the photoelectron spectrum depicted in Fig. 2. In this spectrum we associate the peak of highest kinetic energy with ionization of the vibrationless level $v=0$ in S_0 to the vibrationless level $v^+=0$ in D_0. Such a peak will in the rest of this article be abbreviated as the $0''$-0^+ peak. We determine from the peak's position an adiabatic ionization energy of 10.230 ± 0.015 eV. The spectrum shows furthermore a progression in a vibration with a frequency of 208 meV. This frequency and the intensity distribution over the observable members are in good agreement with the spectra obtained with He(I) excitation[26–28] and with our threshold-resolved photoionization experiments (*vide supra*). Our calculations indicate that, although the vibrational

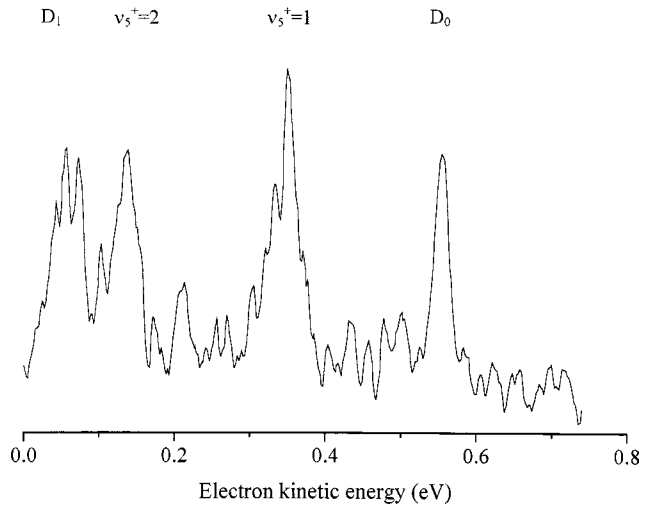

FIG. 2. Kinetic-energy-resolved detection of photoelectrons after direct two-photon ionization of formamide at a one-photon energy of 43 500 cm^{-1}.

frequency found in this experiment and in the threshold ionization experiment match within the experimental error, part of the difference between the 191- and 208-meV values is real. Table II shows that a similar activity is predicted for both ν_4^+ and ν_5^+. The onset of the threshold observed in the threshold experiment is in that case associated with the ν_5^+ threshold and the ν_4^+ threshold cannot be resolved, while in the direct two-photon ionization experiment the photoelectron peaks should in fact be assigned as the nonresolvable peaks to ν_4^+ and ν_5^+ levels, as a result of which these peaks undergo an apparent shift with respect to the threshold experiment.

In the two previous experiments ionization has been performed nonresonantly. In the next section excited-state photoelectron spectroscopy will be performed, i.e., the ionization process will occur resonantly. Also from these experiments an adiabatic ionization energy could be determined. Averaging over the various photoelectron spectra, we find in that case a value of 10.233 ± 0.008 eV. We thus come to the conclusion that the currently determined value for the adiabatic ionization energy supports the value reported previously by Siegbahn *et al.*[28]

In the study by Siegbahn *et al.* a value of 10.699 eV was reported for the vertical ionization energy to D_1. The ionization pattern to D_1 showed a 222-meV progression, and it was therefore suggested that the adiabatic ionization energy is either equal to the vertical ionization energy, or one quantum lower, i.e., 10.477 eV. The spectrum shown in Fig. 2 has a better resolution than the spectrum given in Ref. 28, although not as high a signal-to-noise ratio. From Fig. 2 we determine a vertical ionization energy of 10.725 ± 0.020 eV for D_1. The energy resolution in this part of the spectrum is lower because of the near-zero kinetic energy of the generated photoelectrons. At an energy 222 meV below this peak labeled as D_1 the spectrum does not give evidence for another peak, and we therefore conclude that for D_1 the vertical ionization energy is equal to the adiabatic ionization energy.

C. Excitation and excited-state photoelectron spectroscopy

Figure 3 shows the two- and three-photon resonance enhanced ionization spectra of formamide in the energy range of 61 000–76 000 cm^{-1} (7.56–9.42 eV) presented as overlapping scans over the various dye ranges that have not been corrected for the dye gain curves. The excitation spectra in Fig. 3 have been recorded employing electron detection of all electrons irrespective of their kinetic energies, as well as mass-resolved ion detection. For mass-resolved ion detection we found that the parent ion peak could be detected, but that it was much smaller than fragmentation peaks, in particular that of CHO^+. Monitoring either the parent ion or the dominant fragmentation peaks led, apart from a difference in signal-to-noise ratio, to the same excitation spectrum, which, in turn, was the same as that found with electron detection. This proves that the peaks in our excited-state photoelectron spectra (*vide infra*) derive at least for the major part from ionization of formamide itself, and not from one or more of its fragments.

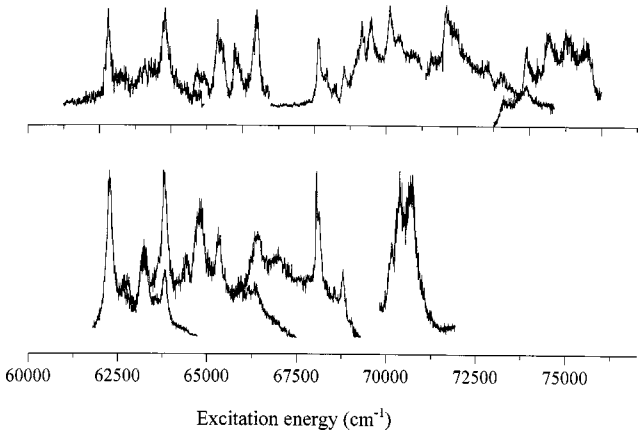

FIG. 3. Multiphoton excitation spectra of formamide in the energy range of 61 000–76 000 cm^{-1} (7.56–9.42 eV). In the upper spectrum resonance enhancement occurs at the two-photon level, in the lower spectrum at the three-photon level.

The multiphoton excitation spectra show various resonances that are given in Table IV. As will be discussed below, excited-state photoelectron spectroscopy enables us to determine a definite assignment of the vibronic nature of the excited state from which ionization took place at these resonances. Consideration of the quantum defect then leads in turn to the assignments that are given in Table IV. About half of these resonances were observed as well in a previous vuv photoabsorption and EEL study[6] where assignments were proposed in terms of Rydberg states converging upon D_0 and D_1. For the lower-energy region—up to the $4s$ Rydberg state—our excited-state photoelectron spectra confirm these assignments, but at the same time they extend our knowledge on the excited-state structure because we observe more resonances. Starting with the $4s$ state, however, our excited-state photoelectron spectra dictate different assignments.

1. 3p Rydberg states

In the following we will show and discuss some of the excited-state photoelectron spectra that bring out the more salient aspects of the spectroscopic and dynamic properties of the excited and ionic states of formamide. Figure 4(a) displays the excited-state photoelectron spectrum of the state reached by two-photon excitation at 62 260 cm^{-1} (7.719 eV). For three-photon excitation a similar spectrum was obtained. The general consensus is that the transition to the vibrationless level of the $^1(3p' \leftarrow n_O)$ state is located here. Since we will not encounter any triplet states in the present study, and because all observed Rydberg states have D_0 as their ionic core, we will in the following abbreviate this state as the $3p'$ state. Considerations, as have been done in the previous sections on the electronic structure of a Rydberg state in relation to its ionic core, make us expect that ionization from this state should predominantly occur to the vibrationless level of D_0. Indeed, we find that the dominant peak in this spectrum has an energy of 1.345 ± 0.010 eV, which, employing an adiabatic ionization energy of 10.233 eV, is readily associated with ionization to the $v^+ = 0$ level starting from a vibrationless ground state. This result thus confirms the previous $[3p']0_0^0$ assignment. As remarked in the precedings section, equally important is that it validates our conclusion concerning the value of the lowest ionization potential.

In the three-photon excitation spectrum a resonance is observed at 63 222 cm^{-1} (7.840 eV), which is much less clear in the two-photon counterpart. vuv-absorption measurements proposed a $[3p'']0_0^0$ assignment, and we expect accordingly a strong $0''\text{-}0^+$ peak in the photoelectron spectrum. This expectation is met by the spectrum depicted in Fig. 4(b) that shows, on the other hand, at the same time that the dominant peak in the spectrum is one that is associated with ionization to an ionic level with 122 meV (984 cm^{-1}) of vibrational energy. Additionally, a small peak is observed that is shifted by 199 meV (1605 cm^{-1}) from the $0''\text{-}0^+$ peak. As in the rest of this article, we will choose to assign peaks at the latter energy to the $\nu_5^+ = 1$ level, but at the same time recall the considerations of the previous sections that tell us that in reality our experimental resolution and the susceptibility of Franck–Condon factors to Duschinsky mixing does not allow us to decide whether this peak should be assigned to the $\nu_5^+ = 1$ or $\nu_4^+ = 1$, or even to both levels. The presence of this peak is perfectly feasible, it just demonstrates that there are slight differences between the $3p''$ state and its ionic core, and that these differences are larger than those for the $3p'$ state, where this ionization pathway was not observed.

The 122-meV peak poses a larger problem. If this peak and the $0'\text{-}0^+$ peak were both to derive from ionization of the vibrationless level of the $3p''$ state, it would imply a huge difference between the equilibrium structure of this state and that of its ionic core, which is at odds with our general ideas on Rydberg states. How can we reconcile the two? We start by noticing that the 122-meV value is within experimental error equal to the energy difference between the present excitation energy and the excitation energy of the vibrationless $3p'$ state (118 meV). Near an energy of 118 meV (948 cm^{-1}) above the $[3p']0_0^0$ transition, a number of vibrational levels are found—the ionic frequencies of Table II indicate levels such as the totally symmetric 8^1 and 9^2 levels, and the nontotally symmetric 10^1 level. Within the Born–Oppenheimer approximation the $[3p']10_0^1$ transition is forbidden, while the $[3p']8_0^1$ and $[3p']9_0^2$ transitions are not expected to carry an intensity on account of their small Franck–Condon factors (see Table III). If there is, however, vibronic coupling between the $[3p'']0^0$ level and these $3p'$ vibrational levels, the wave function of the state that is ionized does not only contain $v' = 0$ but also $\nu'_{10} = 1$, $\nu'_8 = 1$, and $\nu'_9 = 2$ character, the exact composition of the wave function being determined by the various coupling strengths and energy differences. Ionization of this wave function then does not only lead to the formation of vibrationless ions, but also to ions in their $\nu_{10}^+ = 1$, $\nu_8^+ = 1$, and $\nu_9^+ = 2$ states. The peak observed in the photoelectron spectrum at 122 meV from the $0''\text{-}0^+$ peak is thus assigned as deriving from ionization of vibrational levels of the $3p'$ Rydberg state that become accessible by vibronic coupling. The most plausible levels have been mentioned, but we notice that the excited-state photoelectron spectrum does not enable us to distinguish between them. Because of the vibrational state density, it is clear that this vibronic coupling mechanism will only gain in impor-

tance when excitation of higher-lying states is considered. At the same time, the increased vibrational density will more progressively inhibit us to assign specific vibrational levels that are coupled.

Similar patterns are also observed when excited-state photoelectron spectra are taken after excitation of a vibrational level in the excited state. Figure 4(c) shows, for example, the spectrum obtained after two-photon excitation at

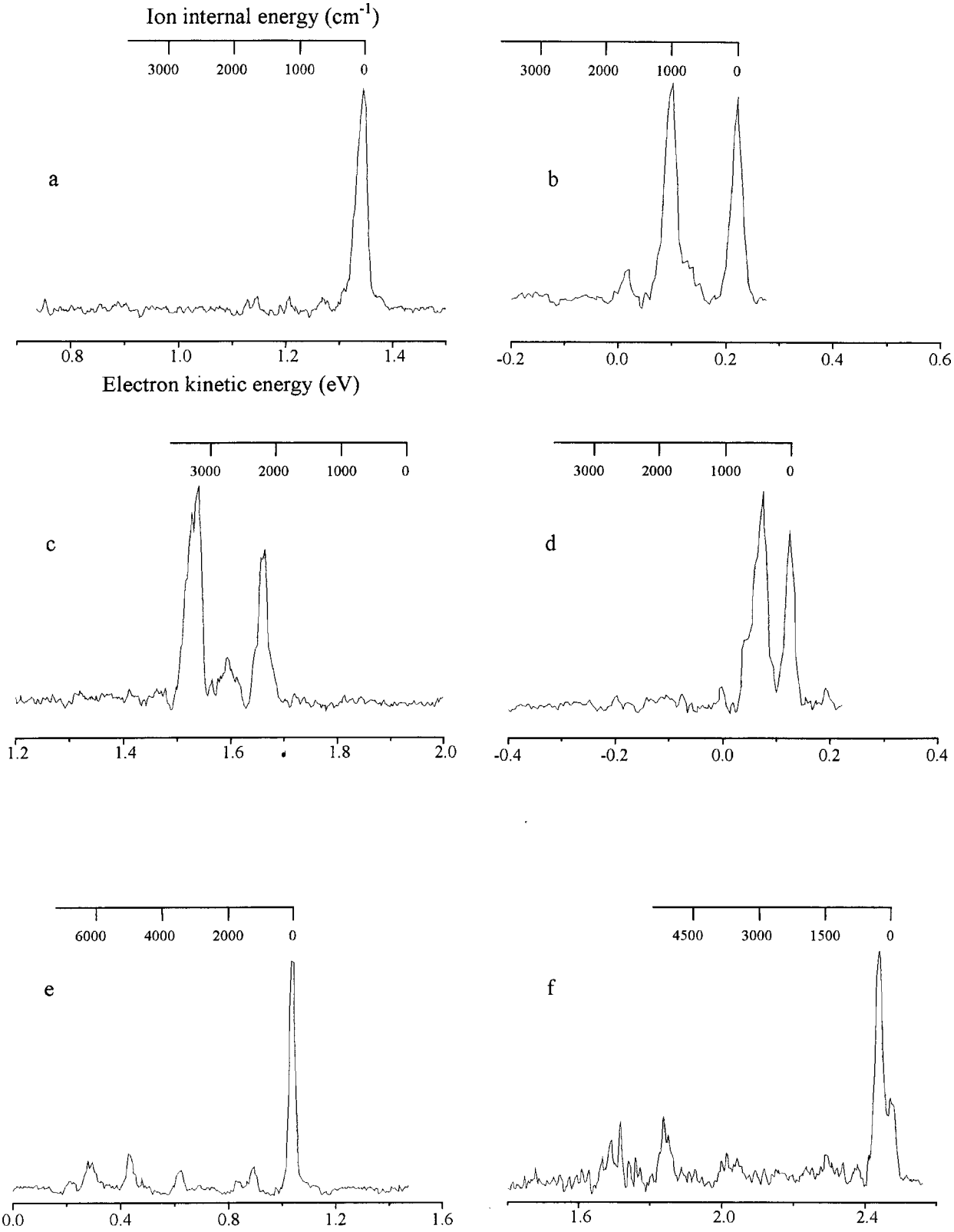

FIG. 4. Excited-state photoelectron spectra obtained after (a) two-photon excitation at 62 260 cm^{-1}, (b) three-photon excitation at 63 222 cm^{-1}, (c) two-photon excitation at 65 330 cm^{-1}, (d) three-photon excitation at 62 682 cm^{-1}, (e) three-photon excitation at 68 128 cm^{-1}, (f) two-photon excitation at 68 360 cm^{-1}, (g) three-photon excitation at 68 832 cm^{-1}, and (h) two-photon excitation at 74 518 cm^{-1}.

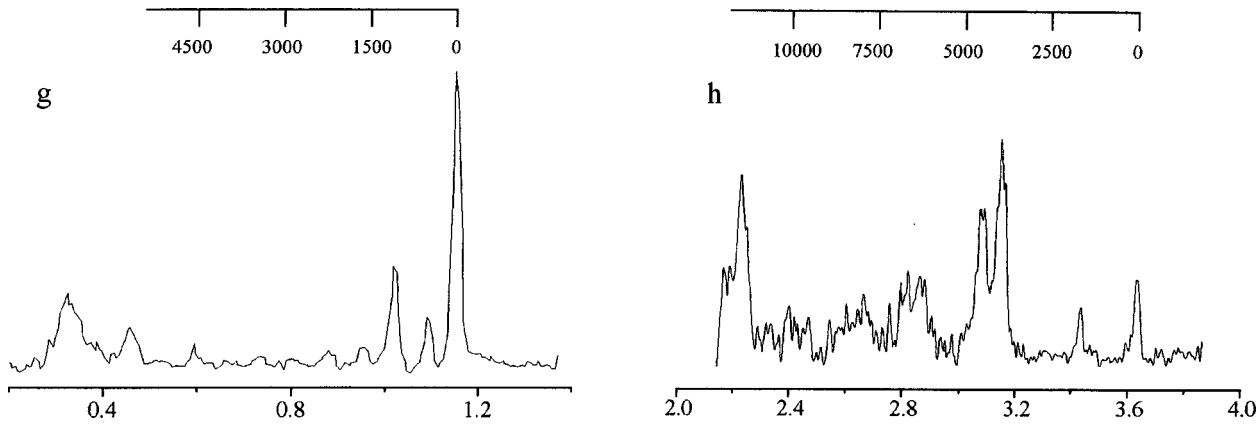

FIG. 4. (*Continued.*)

65 330 cm^{-1}. The dominant peak is located 387 meV (3120 cm^{-1}) from the $0''$-0^+ energy where no peak is observed. This vibrational energy strongly suggests an assignment to the $\nu_5^+=2$ level, and thus that the vibronic level from which ionization took place was a Rydberg state in its $\nu_5'=2$ level. Knowing that the $3p'$ state is located 3070 cm^{-1} below this excitation energy consequently allows us to conclude that the resonance at 65 330 cm^{-1} should be assigned as the $[3p']5_0^1$ transition, in agreement with previous propositions. Interestingly, we notice that the absence of the $0''$-0^+ peak and peaks at the expected positions for ionization to the $\nu_5^+=1$ and 3 levels demonstrate that the spectroscopic properties of the $3p'$ state resemble to a very large extent those of its ionic core.

Apart from the peak at 1.530 eV, two more peaks are observed. The first one at 1.659 eV (258 meV from the $0''$-0^+ position) is readily associated with ionization from vibrational levels of the $3p''$ state whose origin transition is found 2108 cm^{-1} (261 meV) lower in energy. The second peak at 1.596 eV is in the first instance more puzzling. The creation of ions with a vibrational energy of 321 meV (2589 cm^{-1}) suggests that an excited level is ionized with this amount of vibrational energy, and thus the presence of a state at $65\,330-2589=62\,741$ cm^{-1}. In hindsight, we notice that also in Fig. 4(b) a small shoulder can be seen at about 0.129 eV that agrees well with the assumption of a vibrationless state around 62 700 cm^{-1}, and that also in all of our other recorded photoelectron spectra such a shoulder or peak is present. In the excitation spectra of Fig. 3 we observe indeed a peak at 62 682 cm^{-1} with low intensity that perfectly fits the assumption. The excited-state photoelectron spectrum obtained after three-photon excitation is depicted in Fig. 4(d), and shows a peak at the expected $0''$-0^+ position (0.129 eV), as well as a peak with 54 meV vibrational energy that can only be assigned to the $\nu_9^+=1$ level. This peak is attributed to ionization of the $[3p']9^1$ level, which is quasidegenerate with the vibrationless level responsible for the $0''$-0^+ peak. We explicitly notice that the photoelectron spectrum cannot be explained assuming that only the $[3p']9^1$ level is excited: Franck–Condon considerations would then predict a longer progression in ν_9^+, but most of all that the $3p'$ and D_0 states differ considerably, at odds with all other available material, cf. Fig. 4(a). The effective quantum number $(n-\delta)$ of the state located at 62 682 cm^{-1}, 2.35, leaves no doubt that we deal here with one of the three $3p$ states, the other two being the $3p'$ and $3p''$ states at 62 260 and 63 222 cm^{-1}, respectively. In a previous study this state, designated as $3p$, was not observed directly, but from extrapolations deduced to be around 7.40 eV (59 684 cm^{-1}). The present study demonstrates that this assumption should be revised. Now that we have located the 0-0 transition to the $3p$ state, other peaks in the excitation spectra also fall into place. Table IV shows in fact that the complete region from 62 000 up to 67 000 cm^{-1} can be very well explained in terms of transitions to the three $3p$ states with, as expected on the basis of the nonresonantly enhanced photoelectron spectrum in Fig. 2 and the He(I) photoelectron spectrum,[28] for all states, considerable activity of ν_5'.

2. 3d and 4s Rydberg states

Starting from 67 000 cm^{-1}, one may expect states from the $3d$ manifold to appear. The previous vuv absorption study assigned three of such states ($3d$, $3d'$, and $3d''$); our studies confirm these assignments, but reassign the peak previously assigned to the $4s$ state to yet another $3d$ state designated as $3d'''$. For the $3p$ states we observed in the excitation spectra a dominant role of ν_5'. This vibration is also found to be active for the $3d$ states as can be seen from Table IV and Fig. 3. A difference with the $3p$ states is that, apart from this ν_5 vibration, other vibrations are seen as well in the excitation and photoelectron spectra. Consider, for example, the excited-state photoelectron spectrum obtained after three-photon excitation of the $3d'$ state at 68 128 cm^{-1} [Fig. 4(e)]. This spectrum shows as expected a dominant $0''$-0^+ peak. Apart from this peak, peaks are observed displaced by 147, 604, and 748 meV to lower energies, which derive from vibronic coupling with high vibrational states of the $3d$, $3p''$, and $3p'$ states. We notice that in this particular case ionization of the $3p$ levels is not well resolved. The remaining two peaks removed by 201 and 420 meV from the $0''$-0^+ peak cannot be associated with other electronic states and derive therefore from nondiagonal ionization of the $[3d']0^0$ level. The first peak is by now well known and is assigned to the $\nu_5^+=1$ level; the second one we assign on the basis of Table II to the $\nu_2^+=1$ level. The small but visible activity of

TABLE IV. Resonances observed in the two- and three-photon excitation spectra of formamide and their assignments. Indicated in bold are resonances that previously have not been reported or have been assigned differently.

$2h\nu$ (cm^{-1})	$3h\nu$ (cm^{-1})	vuv[a] (eV)	Assignment	$n-\delta$
62 260	62 274	7.72	$[3p']0_0^0$	2.33
	62 740		$[3p]0_0^0$	2.35
63 256	63 222	7.83	$[3p'']0_0^0$	2.38
63 848	63 823	7.92	$[3p']5_0^1$	
	64 428		$[3p]5_0^1$	
64 820	64 821	8.03	$[3p'']5_0^1$	
65 330	65 349	8.10	$[3p']5_0^2$	
65 810		8.16	$[3p]5_0^2$	
66 408	**66 420**	8.21	$[3p'']5_0^2$	
	66 938	8.29	$[3d]0_0^0$	2.66
68 120	68 118	8.44	$[3d']0_0^0$	2.76
68 360			$[3d']12_1^1$	
68 592	**68 573**		$[3d']9_0^1$	
68 832	68 817	8.56	$[3d'']0_0^0$	2.83
69 324			$[3d']7_0^1$	
69 596		8.63	$[3d']5_0^1$	
70 118	**70 157**		$[3d''']0_0^0$	2.97
70 340	70 372	8.74	$[3d'']5_0^1$	
70 670	**70 670**		$[4s]0_0^0$	3.04
71 252			$[3d']5_0^2$	
71 672			$[3d''']5_0^1$	
71 956			$[3d'']5_0^2$	
72 244			$[4s]5_0^1$	
72 684			$[4p']0_0^0$	3.34
72 820			$[4p'']0_0^0$	3.36
73 220			$[3d''']5_0^2$	
73 888			$[4s]5_0^2$	
74 212			$[4d]0_0^0$	3.63
74 518			$[4d']0_0^0$	3.70
75 020			$[4d'']0_0^0$	3.82
75 540			$[4d''']0_0^0$	3.97

[a]Values reported in the vuv absorption study of Ref. 6.

this symmetric N–H stretch vibration indicates that for this particular state the N–H bond lengths are changed upon excitation.

Our calculations predict that $\nu_{12}(a'')$ increases more than twofold upon ionization from the ground state. Since we are dealing here with a vibrational mode of which the frequency in the electronic ground state was in the past difficult to calculate accurately, one might wonder to what extent this prediction is reliable. The transition at 68 360 cm^{-1} seen in the two-photon excitation spectrum as a shoulder on the $[3d']0_0^0$ transition offers us the possibility to investigate this vibration in more detail. Figure 4(f) displays the photoelectron spectrum that results after (2+1) ionization at this energy. It shows a dominant peak that corresponds to the formation of ions with apparently 34 meV (274 cm^{-1}) of vibrational energy. Inspection of Table II tells us that this energy cannot be associated with a totally symmetric vibration if excitation took place from the vibrationless ground state. Assuming that our calculations predict the frequency of ν_{12} in the ionic state completely wrong does not help us either, because then the photoelectron spectrum would force us to conclude that the excited level that is ionized is—within the Born–Oppenheimer approximation, forbidden–a nontotally symmetric vibrational level. The pieces of the puzzle fall into place if we assign the transition to the allowed $[3d']12_1^1$ hot-band transition. In that case we find that the $\nu'_{12}=1$ level is located at 531 cm^{-1}, and the $\nu_{12}^+=1$ level at 74 meV (595 cm^{-1}), in good agreement with our calculations. The other peaks in the photoelectron spectrum at lower kinetic energies have their counterparts in the photoelectron spectrum of Fig. 4(e) and are similarly assigned. The peak at the $0''$-0^+ energy derives from the fact that at this excitation energy we also still excite the $[3d']0^0$ level.

Ionization via the $3d''$ state provides more support for the conclusion that the $3d$ states differ to a larger extent from their ionic core than the $3p$ states. The excited-state photoelectron spectrum obtained after excitation of its vibrationless level at 68 832 cm^{-1} is shown in Fig. 4(g). Our attention concerns now in particular the ionization pathways that lead to ions with a low vibrational content—the peaks at low photoelectron kinetic energy derive from the ionization of high-lying vibrational levels of lower-lying states. Apart from the dominant $0''$-0^+ peak, significant vibrational activity is seen in the form of the peaks at 58 meV (468 cm^{-1}) and 135 meV (1089 cm^{-1}) that we associate with ionization to the $\nu_9^+=1$ and $\nu_8^+=1$ levels, respectively, and some minor activity of ν_5^+ that appears 197 meV (1589 cm^{-1}) from the $0''$-0^+ peak.

The two-photon resonance observed in our study at 70 118 cm^{-1} (8.70 eV) was previously assigned as the vibrationless transition to the $4s$ Rydberg state. The photoelectron spectrum that we observe here (not shown) does indeed reveal a dominant $0''$-0^+ peak in agreement with such an assignment. We run into problems, however, when the photoelectron spectrum obtained at the 70 670-cm^{-1} resonance (not shown) is considered, because it shows a dominant $0''$-0^+ peak as well, and therefore implies that an electronic state is also located at 70 670 cm^{-1}. The effective quantum numbers of the two states, 2.97 and 3.04, suggest that the 70 118-cm^{-1} resonance should be reassigned as one of the states of the $3d$ manifold—we will label this one as the $3d'''$ state—while the 70 670-cm^{-1} resonance is the $4s$ state.

3. Higher excited states

At even higher energies the two-photon excitation spectrum displays some other twelve resonances. At these excitation energies we may anticipate excitation of the $4p$ and $4d$ manifold, but, at the same time, that overlap will occur with transitions to other states that involve ν_5 since the energy differences between the various states are getting smaller now. The photoelectron spectrum recorded at a certain excitation energy gives therefore general evidence for the presence of various states from which ionization occurred. As an example, we show in Fig. 4(h), the photoelectron spectrum that results from two-photon excitation at 74 518 cm^{-1}. At the predicted $0''$-0^+ position of 3.638 eV a peak is seen that would imply a vibrationless level character of the state that is ionized. Based on the quantum defect, we assign the resonance at this energy, in part, to the $[4d']0_0^0$ transition. Another peak is observed at 199 meV higher internal energy. This peak implies $\nu_5=1$ character at the two-photon level and is therefore concluded to derive from ionization of the $[4p'']5^1$ level, predicted to be located as well

near this excitation energy. At even lower photoelectron kinetic energies, i.e., at higher internal energies of the ion, a plethora of peaks is seen that can be assigned without difficulty to ionization of high-lying vibrational levels of lower-lying Rydberg states. That these peaks are in general more intense than the two peaks discussed previously is because the former peaks are associated with states with a lower principal quantum number; they therefore have a higher ionization cross section.

Table IV shows that for the $3p$ and $3d$ Rydberg manifold the present assignments based on measured photoelectron spectra are *grosso modo* in agreement with those reached in the vuv absorption study.[6] In that study, higher-lying Rydberg states were assigned using the Rydberg formula, employing for the ionization energy a value of 10.13 eV. Here we have concluded that this value is not correct; in fact, our value of 10.233 ± 0.008 eV reproduces that of 10.229 eV reported by Siegbahn *et al.*[28] Since the vuv study proposed assignments basically by grouping features with the same quantum defect, we may expect that most of the features observed in the vuv study at higher excitation energies need to be reassigned, as is partly confirmed by our measurements in the 70 500–75 500-cm^{-1} region.

In a recent *ab initio* study,[51] calculations have been performed on the excitation energies and one-photon transition dipole moments of the excited states of formamide. These studies predict for the $3s$ and $3p$ Rydberg states that those with the $(n_O)^{-1}$ ionic core are located at higher vertical excitation energies than the ones with the $(2\pi)^{-1}$ ionic core. In particular, it would appear as if the strongest of the absorption features at 7.72 eV (62 260 cm^{-1}) is associated with the $3p_\pi \leftarrow 2\pi$ excitation. The vuv study[6] argued already that this feature is linked to the D_0 state on the basis of the observed vibrational structure, the present study confirms and extends this conclusion. First, the photoelectron spectra demonstrate unambiguously that the ionic core of the Rydberg state is D_0 and not D_1. Second, our *ab initio* calculations predict that D_0 should be assigned as $(n_O)^{-1}$ and not as $(2\pi)^{-1}$ and confirm the observed vibrational activity in He(I) photoelectron spectra (*vide supra*). Additionally, we have performed a time-dependent DFT calculation[52] of the excitation energies of the excited states of the formamide radical cation at the UB3LYP/6-311+G* level and find here that D_1 is the $1\,^2A''(2\pi)^{-1}$ state. At the equilibrium geometry of S_0 this state is removed by 0.37 eV from the $X\,^2A'(n_O)^{-1}$ state, in perfect agreement with the experimental difference in vertical ionization energies of 0.25 eV.

The present study has provided an extensive description of the spectroscopic and dynamic properties of the Rydberg manifold converging upon the lowest ionic state. On the basis of the energy difference between D_0 and D_1, one would *a priori* expect that in the currently investigated energy region also Rydberg states converging upon D_1 are located. In fact, already some time ago the absorption spectrum in the $3p$ region (7.7–8.7 eV) was compared with the band envelopes of D_0 and D_1 in the photoelectron spectrum.[26] From the close correspondence between the two, it was concluded that the $3p \leftarrow 2\pi$ band was about 4000 cm^{-1} higher than the $3p \leftarrow n_O$ band. The previous vuv absorption study attempted similarly to propose assignments for some of the observed features in terms of Rydberg states with a D_1 ionic core. Our photoelectron spectra, on the other hand, do not give any indication that at some point we are exciting $(2\pi)^{-1}$ Rydberg states. A possible reason might be that the two- and/or three-photon excitation cross section of $(2\pi)^{-1}$ Rydberg states is considerably smaller than that of $(n_O)^{-1}$ Rydberg states, or that Rydberg states with the $(2\pi)^{-1}$ ionic core are subject to rapid decay processes such as predissociation.

IV. CONCLUSIONS

We have investigated the Rydberg and ionic manifold of formamide by a combination of experimental and theoretical methods. As far as the ionic manifold is concerned, we have demonstrated by various experimental approaches that the adiabatic ionization energy of 10.13/10.15 eV employed so far in other experimental studies is not correct. We find a value of 10.233 ± 0.008 eV that reproduces the value reported by Siegbahn *et al.*[28] The improved resolution in our direct two-photon ionization experiments has enabled us to conclude that the adiabatic ionization threshold of the first excited state of the radical cation is located at 10.725 ± 0.020 eV and not 222 meV lower as was still possible to conclude from previous experiments. Our calculations on the state ordering in the radical cation, and the nice agreement between calculated and observed Franck–Condon factors have firmly established that the ground and first excited states of the radical cation are associated with the removal of an electron from the n_O and 2π orbital, respectively.

Application of excited-state photoelectron spectroscopy on excited states in the 7.6–9.4-eV energy region that were populated by two- and/or three-photon excitation has led to an unambiguous assignment of the various resonances present in the excitation spectra. These studies have allowed us to chart out a large part of the Rydberg manifold that was previously not firmly assigned. In fact, from these studies it has become clear that a large part of previously proposed assignments needs to be revised, and that in the present study new states have been observed. The spectroscopic properties of the Rydberg states resemble closely those of their ionic core: it is mainly the ν_5 vibration that is observed to be active. Interestingly, our calculations show that this vibration changes considerably in character upon excitation. Our photoelectron spectra demonstrate that the dynamic properties of the investigated Rydberg states are dominated by vibronic coupling. As a result, we observe not only ionization of the ''bright'' state that is excited, but also of ''dark'' high-lying vibrational levels of lower-lying excited states that are not accessible by direct excitation from the electronic ground state.

ACKNOWLEDGMENTS

Part of this work was supported by the European Community (TMR Contract No. ERBFMRXCT970097). The authors wish to thank Ing. D. Bebelaar for valuable experimental assistance, and Professor C. A. de Lange and Professor M. Glasbeek for use of equipment.

[1] D. A. Leigh, A. Murphy, J. P. Smart, and A. M. Z. Slawin, Angew. Chem. Int. Ed. Engl. **36**, 728 (1997).
[2] D. A. Leigh and A. Murphy, Chem. Ind. **178**, (1999).
[3] V. Bermudez, N. Capron, T. Gase, F. G. Gatti, F. Kajzar, D. A. Leigh, F. Zerbetto, and S. Zhang, Nature (London) **406**, 608 (2000).
[4] A. M. Brouwer, C. Frochot, F. G. Gatti, D. A. Leigh, L. Mottier, F. Paolucci, S. Roffia, and G. W. H. Wurpel, Science **291**, 2124 (2001).
[5] M. Asakawa, G. Brancato, M. Fanti, D. A. Leigh, T. Shimizu, A. M. Z. Slawin, J. K. Y. Wong, F. Zerbetto, and S. W. Zhang, J. Am. Chem. Soc. **124**, 2939 (2002).
[6] J. M. Gingell, N. J. Mason, H. Zhao, I. C. Walker, and M. R. F. Siggel, Chem. Phys. **220**, 191 (1997).
[7] J. C. Evans, J. Chem. Phys. **22**, 1228 (1954).
[8] S. T. King, J. Phys. Chem. **75**, 405 (1971).
[9] K. Itoh and T. Shimanouchi, J. Mol. Spectrosc. **42**, 86 (1972).
[10] M. Räsänen, doctoral thesis, University of Helsinki, 1983.
[11] M. Räsänen, J. Mol. Struct. **101**, 275 (1983).
[12] J. Lundell, M. Krajewska, and M. Räsänen, J. Phys. Chem. A **102**, 6643 (1998).
[13] L. Z. Stenkamp and E. R. Davidson, Theor. Chim. Acta **44**, 405 (1977).
[14] C. W. Bock, M. Trachtmann, and P. J. George, Mol. Spectrosc. (Chem. Soc., London) **89**, 76 (1981).
[15] G. Fogarasi and A. Balázs, J. Mol. Struct.: THEOCHEM **133**, 105 (1985).
[16] R. J. Kurland, J. Chem. Phys. **23**, 2202 (1955).
[17] R. J. Kurland and E. B. Wilson, J. Chem. Phys. **27**, 585 (1957).
[18] C. C. Costain and J. M. Dowling, J. Chem. Phys. **32**, 158 (1960).
[19] E. Hirota, R. Sugisaki, C. J. Nielsen, and O. Sørensen, J. Mol. Spectrosc. **49**, 251 (1974).
[20] M. Kitano and K. Kichutsu, Bull. Chem. Soc. Jpn. **47**, 67 (1974).
[21] R. D. Brown, P. D. Godfrey, and B. Kleibömer, J. Mol. Spectrosc. **124**, 34 (1987).
[22] M. W. Wong, K. B. Wiberg, and M. J. Frisch, J. Am. Chem. Soc. **114**, 1645 (1992).
[23] G. Fogarasi and P. G. Szalay, J. Phys. Chem. A **101**, 1400 (1997).
[24] H. Basch, M. B. Robin, and N. A. Kuebler, J. Chem. Phys. **49**, 5007 (1968).
[25] A. Lisini, M. P. Keane, S. Lunell, N. Correia, A. Naves de Brito, and S. Svensson, Chem. Phys. **169**, 379 (1993).
[26] C. R. Brundle, D. W. Turner, M. B. Robin, and H. Basch, Chem. Phys. Lett. **3**, 292 (1969).
[27] K. Kimura, S. Katsumata, Y. Achiba, T. Yamazaki, and S. Iwata, *Handbook of Photoelectron Spectra of Fundamental Organic Molecules* (Japan Scientific Societies, Tokyo, 1981).
[28] H. Siegbahn, L. Asplund, P. Kelfve, K. Hamrin, L. Karlsson, and K. Siegbahn, J. Electron Spectrosc. Relat. Phenom. **5**, 1059 (1974).
[29] H. D. Hunt and W. T. Simpson, J. Am. Chem. Soc. **75**, 4540 (1953).
[30] K. Kaya and S. Nagakura, Theor. Chim. Acta **7**, 117 (1967).
[31] R. A. Rijkenberg and W. J. Buma, J. Phys. Chem. A **106**, 3727 (2002).
[32] D. H. A. ter Steege, A. C. Wirtz, and W. J. Buma, J. Chem. Phys. **116**, 547 (2002).
[33] R. A. Rijkenberg, W. J. Buma, C. A. van Walree, and L. W. Jenneskens, J. Phys. Chem. A **106**, 5249 (2002).
[34] C. R. Scheper, W. J. Buma, and C. A. de Lange, J. Electron Spectrosc. Relat. Phenom. **109**, 8319 (1998).
[35] A. M. Rijs, E. H. G. Backus, C. A. de Lange, N. P. C. Westwood, and M. H. M. Janssen, J. Electron Spectrosc. Relat. Phenom. **112**, 151 (2000).
[36] P. Kruit and F. H. Read, J. Phys. E **16**, 313 (1983).
[37] C. E. Moore, Atomic Energy Levels, Natl. Bur. Stand. (U.S.) circ. No. 35 (U.S. GPO, Washington, D.C., 1971), Vol. II.
[38] C. Lee, W. Yang, and R. G. Parr, Phys. Rev. B **37**, 785 (1988).
[39] A. D. Becke, Phys. Rev. A **38**, 3098 (1988).
[40] B. Miehlich, A. Savin, H. Stoll, and H. Preuss, Chem. Phys. Lett. **157**, 200 (1989).
[41] A. D. Becke, J. Chem. Phys. **98**, 5648 (1993).
[42] E. D. Simandiras, J. E. Rice, T. J. Lee, R. D. Amos, and N. C. Handy, J. Chem. Phys. **88**, 3187 (1988).
[43] R. Krishnan, J. S. Binkley, R. Seeger, and J. A. Pople, J. Chem. Phys. **72**, 650 (1980).
[44] A. D. McLean and G. S. Chandler, J. Chem. Phys. **72**, 5639 (1980).
[45] M. J. Frisch, G. W. Trucks, H. B. Schlegel *et al.*, GAUSSIAN 98, Revision A.5, Gaussian, Pittsburgh, PA, 1998.
[46] W. J. Buma and F. Zerbetto, J. Chem. Phys. **103**, 10492 (1995).
[47] J. M. Zwier, P. G. Wiering, A. M. Brouwer, D. Bebelaar, and W. J. Buma, J. Am. Chem. Soc. **119**, 11523 (1997).
[48] J. M. Zwier, A. M. Brouwer, R. A. Rijkenberg, and W. J. Buma, J. Phys. Chem. A **104**, 729 (2000).
[49] G. Balakrishnan, T. Keszthelyi, R. Wilbrandt, J. M. Zwier, A. M. Brouwer, and W. J. Buma, J. Phys. Chem. A **104**, 1834 (2000).
[50] J. M. Zwier, A. M. Brouwer, W. J. Buma, A. Troisi, and F. Zerbetto, J. Am. Chem. Soc. **124**, 149 (2002).
[51] M. E. Casido, C. Jamorski, K. C. Casido, and D. R. Salahud, J. Phys. Chem. **108**, 4439 (1998).
[52] J. D. Hirst, D. M. Hirst, and C. L. Brooks III, J. Phys. Chem. **100**, 13487 (1996).
[53] A. P. Scott and L. Radon, J. Phys. Chem. **100**, 16502 (1996).